# DUCTILE-BRITTLE TRANSITIONS IN THE FRACTURE OF PLASTICALLY-DEFORMING, ADHESIVELY-BONDED STRUCTURES: II NUMERICAL STUDIES

C. Sun[a], M.D. Thouless[b, c], A.M. Waas[a, b], J.A. Schroeder[d] and P.D. Zavattieri[d]

[a]*Department of Aerospace Engineering, University of Michigan, Ann Arbor, MI 48109, USA*

[b]*Department of Mechanical Engineering, University of Michigan, Ann Arbor, MI 48109, USA*

[c]*Department of Materials Science and Engineering, University of Michigan, Ann Arbor, MI 48109, USA*

[d]*General Motors Research and Development, 30500 Mound Rd., Warren, MI 48090, USA*

## ABSTRACT

To enable the effective and reliable use of structural adhesive bonding in automotive applications, the cohesive properties of a joint need to be determined over a wide range of loading rates. In this paper, a strategy for determining these properties has been described and used to analyze a set of experimental results presented in a companion paper. In the particular system studied, a crack growing in a toughened quasi-static mode could make a catastrophic transition to a brittle mode of fracture. The cohesive parameters for both the toughened and brittle modes of crack growth were determined by comparing numerical predictions from cohesive-zone simulations to the results of experimental tests performed using double-cantilever beam specimens and tensile tests. The cohesive parameters were found to be essentially rate independent for the toughened mode, but the toughness dropped by a factor of four upon a transition to the brittle mode. The results of wedge tests were used as an independent verification of the cohesive parameters, and to verify that the quasi-static properties remained rate-independent to very high crack velocities corresponding to conditions of low-velocity impact. The effects of friction, and the use of the wedge test to determine cohesive parameters, were also explored.

(February 6, 2008)

## 1. Introduction

While the use of structural adhesives has great potential for the automotive industry, especially in the construction of light-weight vehicles, a major obstacle to their use are insufficiently developed design methodologies and characterization techniques. Structural joints for automotive applications need to deform plastically to ensure optimal levels of energy absorption during a crash. Therefore, of particular importance is an ability to characterize the properties of plastically-deforming adhesive joints under different rates of loading. It is well-recognized that adhesive joints that deform elastically can be characterized by the tools of mixed-mode fracture mechanics, with a toughness that depends on the thickness of the adhesive layer, the rate of testing and the mode of loading. However, these traditional tools of fracture mechanics, which depend on assumptions of elastic deformations, cannot be assumed to be applicable for crash conditions in automotive structures.

Numerical analyses using cohesive-zone models for modeling adhesive layers bonding elastic adherends was first presented by Ungsuwarungsri and Knauss (1987), and Tvergaard and Hutchinson (1994; 1996). Yang *et al.* (1999) showed that it was possible to determine from experiments two dominant cohesive parameters that characterize an adhesive layer in a plastically-deforming joint - the cohesive strength and toughness - and to use these values for quantitative predictions. Subsequently work also explored the use of experimental observations to deduce cohesive parameters for adhesive joints. For example, Sørensen (2002), Sørensen *et al*. (2003), and Andersson and Stigh (2004) used the inverse *J*-integral technique of Li *et al.* (1987), to determine the full traction-

separation curve of the adhesive layer. This approach has the advantage of giving the full traction-separation curve in a rigorous fashion when the adherends deform in an elastic fashion. The approach is not valid when the adherends deform plastically; nor is it obvious that cohesive properties obtained under linear-elastic conditions must remain constant when small-scale yielding conditions are violated. Indeed, Cavalli and Thouless (2001) and Andersson and Biehl (2006) have provided specific examples where cohesive parameters appear to change with the deformation of the adherends. Many of the techniques proposed to obtain the cohesive parameters of the adhesive layer when the adherends deform plastically follow the general approach of Yang *et al*. (1999), comparing different experimental features to results of numerical calculations in both mode-I (Ferracin *et al*., 2003; Andersson and Biehl, 2006) and mixed-mode conditions (Yang and Thouless, 2001; Madhusdhana and Narasimhan, 2002; Su *et. al*. 2004; Andersson and Biehl 2006).

In order for cohesive-zone models to be adopted within the automotive industry, the effects of loading rate must be incorporated into the analyses along with the effects of plastic deformation in the sheet metal. Generally an assumption is made that, since polymers are rate sensitive, the behavior of adhesives must also be rate sensitive. This rate sensitivity can then lead to a rich behavior including ductile-brittle transitions and stick-slip fracture (Maugis, 1985). While some rate-dependent cohesive-zone models have been developed (Landis *et al.*, 2000; Rahulkumar *et al.*, 2000; Kubair *et al.*, 2005; Zhou *et al.,* 2005) that may be useful in these applications, measurements of a rate-dependent toughness have generally been limited to those obtained from linear-elastic fracture-mechanics tests (Williams, 1984). As discussed above, there is evidence that the

toughness can be affected by the extent of plasticity. However, even in systems where the toughness might not be affected by changes in constraint associated with large-scale plasticity (Blackman *et al.*, 2000), the cohesive strength is also expected to have some influence on the fracture when the adherends deform plastically (Yang *et al.*, 1999; Ferracin et al 2003; Madhusdhana and Narasimhan, 2002; Su *et. al*. 2004; Andersson and Biehl 2006). Therefore this quantity also needs to be determined and incorporated into the analyses. One of the goals of the research described in this paper is to establish a methodology to obtain mode-I cohesive parameters over a wide range of loading rates which doesn't require assumptions to be made either about the relative importance of the cohesive strength and toughness on fracture behavior, or about whether LEFM values of toughness can be used when the joints deform plastically.

A companion paper (Sun *et al.*, 2008) has presented the results of an experimental study of the fracture of joints consisting of a commercial rubber-toughened adhesive bonding thin sheets of a dual-phase steel. The dimensions of the joints, and the properties of the materials, were such that plastic deformation of the adherends always accompanied fracture. These experiments form the basis of the tests analyzed in this current paper, and were used to determine the cohesive parameters at different loading rates. Two distinct modes of crack growth were identified in these systems: quasi-static crack growth, apparently associated with a tough mode of crack growth, and dynamic fracture, apparently associated with a substantially more brittle mode of crack growth. At low loading rates, only the tougher, quasi-static mode of fracture was observed. At higher loading rates, transitions between quasi-static and dynamic fracture were observed. Quasi-static crack growth could, without any obvious precursor warnings

(such as changes in velocity), change to the lower-toughness mode of crack growth. This transition appeared to be stochastic in nature, with no obviously quantitative features that would allow a simple deterministic model to be developed. While the results of this study will allow some comments to be made about the possible physics behind the transition, the transition *per se* was not modeled in the present study. The goal of this project was initially limited to determining the appropriate cohesive laws for each mode of crack growth, as the first step in developing a methodology for design-level predictions of the effect of loading rate on the performance of structural adhesive joints for automotive applications.

## 2. Numerical Modeling

The development of the particular mode-I cohesive-zone model used in this study is detailed in previous work done by the authors (*e.g.*, Yang *et al.,* 1999; Li *et al.*, 2005a). In particular, it should be noted that the division between the material associated with the cohesive zone and the material associated with the continuum properties of the joint has been made at the adhesive / adherend interface. In other words, all the deformation in the adhesive is assigned to the cohesive zone[1]. The energy dissipated within the adhesive layer (the area under the traction separation law for the adhesive) is described as the toughness of the joint. The maximum tractions that act on the adhesive/metal interface are described as the cohesive strength of the joint. It is appreciated that this approach does not permit predictions of constraint effects that might be associated with changing

[1] In adhesives and other polymers in which the creation of new surfaces is accompanied by extensive deformation and molecular pull-out, rather than being associated with an atomically thin cleavage plane, any internal division of the fracture process into a "cohesive zone" and a "deformation zone" will necessarily be arbitrary. There may be mechanics questions that can be addressed by choosing different scales for this division, but the arbitrary nature of any such choice should always be recognized.

the thickness or material of the adherends. However, for automotive design, it would not seem to be an undue burden to characterize an adhesive in relation to one set of materials, adhesive thickness, and sheet-metal thickness; such an approach substantially minimizes the computational and experimental complications associated with characterization and design. Over the last few years, experimental evidence has strongly indicated that accurate predictions of the performance of different joint geometries can be produced with this approach (Yang *et al.*, 1999; Su *et al.* 2004; Andersson and Sigh, 2004; Li *et al.*, 2005a).

The tractions transmitted across the adhesive layer are related to the opening displacement of the layer through a traction-separation law. This traction-separation law is incorporated within user-defined elements that replace the adhesive along the entire interface. The appropriate traction-separation laws need to be determined by comparison of numerical predictions to experimental observations. Although the details of the laws may have varying degrees of influence on some aspects of cohesive-zone calculations (Chandra *et al.*, 2002; Li and Chandra, 2003; Li *et al.*, 2005b, Alfano, 2006), numerical studies have confirmed that these issues do not have a significant influence on the results presented here. Therefore, the two essential parameters that are focused on in this study are the toughness and the cohesive strength. The general form of the mode-I cohesive law used for the purposes of this study is shown in Figure 1, with the cohesive strength represented as $\hat{\sigma}$, and the toughness (area under the curve) represented as $\Gamma_I$. The shape of this law has been chosen to provide a reasonable approximation to the elastic-plastic deformation of an adhesive layer that is seen as the physically appropriate interpretation of the interfacial bonding. The initial slope was chosen as an approximate match to the

compliance of the constrained adhesive layer, based on continuum calculations of the geometry using the constitutive properties of the adhesive described in the companion paper (Sun *et al.*, 2008). The unloading slope was chosen to be as steep as possible, while minimizing numerical instabilities. The cohesive strength and toughness were determined by comparisons with experimental observations, as discussed in the subsequent sections. Issues of mesh sensitivity were explored to ensure that the results quoted were mesh independent to within a level of uncertainty consistent with the experimental uncertainty.

Experience in earlier studies has indicated that the numerical predictions for different geometries and material combinations can have different sensitivities to the two cohesive parameters. The behavior of some geometries and materials may be described by a distinct pair of toughness and cohesive strength values; the behavior of other geometries by a wider range of complementary pairs of toughness and cohesive strength. In particular, there may be more than one set of cohesive parameters that allow the characteristics of one particular geometry to be modeled, while the performance of other geometries may be insensitive to variations in one of the two parameters. Therefore, as outlined below, an essential aspect of the process for determining the appropriate cohesive parameters is a sensitivity analysis for each test geometry and set of materials used, to make sure that each parameter can be determined independently to within a range of uncertainty consistent with the specimen-to-specimen variation. A final validation step with a separate geometry is also required to confirm the parameters.

## 3. Determination of quasi-static fracture parameters

Numerical models of the double-cantilever-beam (DCB) geometry described in the companion paper (Sun *et al.*, 2008) were conducted using the ABAQUS/Standard 2D finite-element program. Since the loading and crack path were symmetrical, a half geometry was used, with a symmetry plane along the center of the adhesive (Fig. 2). The adhesive was replaced with cohesive elements of thickness 0.4 mm - half the thickness of the adhesive layer. In this context, it should be noted that all values of toughness quoted in this paper represent the toughness of the entire layer (double the toughness of the half thickness represented by the cohesive elements). The other dimensions matched the dimensions of the experimental geometry. The properties of the steel adherends were described by a rate-independent[2], point-to-point representation of the stress-strain curves for the steel, as given in Sun *et al.* (2008). Isotropic properties, with a von Mises yield criterion were assumed for the sheet metal.

Different values of toughness and strength were used for the traction-separation law shown in Fig. 1, and the resultant numerical load-displacement curves were compared to the experimental results obtained in Sun *et al*. (2008) for quasi-static crack growth, over the full range of displacement rates for which this type of crack growth was observed (0.1 mm/s to 200 mm/s). These calculations showed that the numerical results for this geometry (and set of adherends) were relatively insensitive to the value chosen for the cohesive strength of the adhesive layer. As shown in Fig. 3, the agreement

[2] The effects of the small rate-dependence exhibited by the steel were explored numerically using the range of properties exhibited. Within the range of behavior documented in Sun *et al*. (2008), the effects were negligible compared to any experimental uncertainty or variation. Therefore, for computational ease, the rate effects were neglected. Throughout the study, strain rates associated with any plastic deformation were monitored to ensure that the strain-rate did not exceed the range for which these assumptions would be valid.

between the numerical results and the experimental results for the DCB geometry were essentially controlled by the value of toughness, except at very low values of cohesive strength. Furthermore, as discussed in the companion paper, there was no systematic effect of loading rate on the experimental load-displacement curves obtained from this geometry. Therefore, the range of parameters shown in Fig. 3 provide an acceptable description for all the quasi-static results, without regard to applied displacement rate. This notion of rate-independence (that, within the limits associated with specimen-to-specimen variability, this range of parameters described all quasi-static crack growth at velocities in the range of 0.07 to 140 mm/s) was unambiguous, despite evidence of rate dependence for the bulk adhesive over a comparable range of strain rates (Sun *et al.,* 2008)[3].

It will be observed from Fig. 3 that the results for the DCB experiments could be matched numerically using a relatively narrow range of toughness values. However, there was a slight dependence of toughness on the assumed cohesive strength (to a level beyond what was considered to be the range of experimental uncertainty), especially at low values of cohesive strength. Furthermore, there is no reason to expect the relative insensitivity of toughness on cohesive strength to be replicated for other geometries. Therefore, the development of any protocol for determining the cohesive parameters of an adhesive joint, will require that additional geometries with different sensitivities to the two parameters be explored.

[3] Additional numerical continuum models were also conducted for this geometry, using continuum elements for the adhesive layer with the constitutive properties determined in the companion paper, and an assumption of a pressure-independent von Mises yield criterion for the adhesive. These indicated that the strain rates experienced by the adhesive layer in the DCB geometry were in the range of 0.0015 $s^{-1}$ to 3 $s^{-1}$, for crack velocities in the range of 0.07 mm/s to 140 mm/s.

A second geometry suitable for this particular system was designed numerically so that it was much more sensitive to strength than to toughness. The design is illustrated in Fig. 4. Coupons of the dual-phase steel sheet, 40 mm long and 25 mm wide, were bonded over a length of 5 mm. This bond was of the same thickness, and prepared in the same way as all the other bonds in the experimental studies. Beyond the adhesive region, thick "L" arms of steel were bonded symmetrically to the coupons, to provide a means of loading the joint by a pin. The intent of this design was to provide direct tension to the adhesive layer, but to leave it subject to a constraint applicable to sheet metal. Seven specimens were pulled apart at nominal cross-head displacement rates of 0.01 mm/s, 0.1 mm/s and 200 mm/s. Failure in all cases was through the middle of the adhesive, consistent with the failure mechanisms seen for all the mode-I tests described in the companion paper. The nominal strength of the bond was determined by dividing the maximum load supported by the area of the adhesive. This quantity was essentially constant over the entire range of strain rates, and equal to $24 \pm 3$ MPa, with no dependence on rate.

Cohesive-zone analyses were used to examine how the nominal strength for this particular geometry and set of materials depended on the toughness and cohesive strength of the interface. The calculated values of the nominal strength were then compared to the experimental results to deduce the range for both cohesive parameters that would provide a satisfactory fit to the experiments. This range has been superimposed on Fig. 3. As can be seen from this plot, the toughness has no influence on the fit[4]. Furthermore, in this

[4] This statement is valid for the range of toughnesses considered in these particular calculations, which was based on the results from the DCB tests. A toughness dependence would be expected for very brittle

particular system, the cohesive strength was equal to the nominal strength of the bond. This is consistent with a geometry that is loaded in a nominally uniform fashion and with a cohesive-zone length that is much larger than the bond length, so that the stresses in the adhesive layer are essentially uniform.

The value of cohesive strength for the adhesive layer (24 ± 3 MPa) obtained from the preceding analysis was compared to the strength that might have been expected from the ultimate tensile strength of the bulk adhesive. A numerical continuum analysis of the geometry was conducted using continuum elements to represent the adhesive layer, with the constitutive properties given in the companion paper (Sun *et al*., 2008), and an assumption of a pressure-independent von Mises yield criterion. These calculations indicated that the applied displacement rates of 0.01 mm/s to 200 mm/s corresponded to strain rates in the adhesive of 0.013 $s^{-1}$ to 250 $s^{-}1$. They also indicated that a failure criterion based on the ultimate tensile strengths would have predicted nominal bond strengths between 30 and 40 MPa, with a dependence on loading rate that would have been significant beyond the experimental uncertainties. While the cohesive strength deduced from the bonded configuration is consistent with this expected range, it is significantly lower and, as noted earlier, shows no rate dependence. This contrast indicates that the small hydrostatic constraint of the geometry that was noted in the numerical calculations may be triggering failure slightly earlier than in the bulk tests. It also indicates the imperative of obtaining cohesive parameters directly from bonded joints with an appropriate level of constraint, rather than assuming that the parameters are unique, well-defined characteristics of the adhesive alone.

---

systems. In general, the two plots that make up Fig. 3 would be calculated in conjunction with each other, since each might motivate the potential range of parameters for the other.

The fit between the experimental results and the numerical results using these values of cohesive parameters ($\Gamma_I = 4.2 \pm 0.3$ kJ/m$^2$ and $\hat{\sigma} = 24 \pm 3$ MPa) can be seen in Fig. 5. This figure shows the relationship between load and applied displacement for the quasi-static DCB geometry. A further indication of consistency between the numerical model and the experimental results can be obtained by comparing the numerical predictions of the crack velocity with the observed velocities. In the numerical analyses, the crack tip is defined as the point at which the displacement of the cohesive zone model equals $\delta_c$. As can be seen from Fig. 6, the cohesive-zone model does a good job of predicting how the crack length depends on displacement over the entire range of quasi-static experiments. This figure also indicates that the quasi-static crack velocity can be correctly described for this system by the rate-independent cohesive parameters described above since, in a quasi-static model of the type developed here, the crack velocity will scale with the displacement rate only if the cohesive parameters are rate independent.

**4. Determination of dynamic fracture parameters**

The experimental results indicated that there were two modes of crack growth: a toughened mode corresponding to quasi-static crack growth, and a brittle mode. The transition from the toughened to the brittle mode appeared to be stochastic in nature, with an increased likelihood of occurrence at higher velocities. Once the brittle mode of crack growth was triggered, the crack propagated dynamically until equilibrium was restored. Once the crack came to rest, the toughening mechanism appeared to operate again, with the next increment of crack growth occurring in a quasi-static mode. The apparently random transitions to the brittle mode, coupled with the absence of any observable rate-dependence in the cohesive parameters, complicate the development of any mechanistic

model of the transition. It is possible that a brittle-to-tough transition might also be randomly associated with different properties along the adhesive bond. However, while the transition cannot yet be modeled, the crack growth can be analyzed by invoking the assumption that once the brittle mode has been randomly triggered, the strain rate at the tip of a dynamically growing crack is too fast to allow the toughening mechanisms in the adhesive to operate. With this assumption, the tougher mode can occur again only when the dynamic crack has been brought to rest. In this section, it will be shown that once the cohesive parameters for the brittle mode of crack growth have been determined, the return of the toughened mode of crack growth can be predicted.

The cohesive parameters for the brittle mode of crack growth were found using numerical models of the DCB geometries that exhibited both brittle and toughened regions of crack growth, and matching the numerical results to experimental observations. In this context, it should be noted that dynamic fracture in these experiments always occurred after quasi-static crack growth, and the associated plastic deformation of the adherends. Modeling the dynamic portion of crack growth requires that the prior quasi-static portion of the crack growth be correctly incorporated in the analysis. Therefore, the numerical model of the DCB geometries had to contain two zones, each with its own distinct set of cohesive elements. One set of elements was used to model the interface over the initial portion of the specimen where quasi-static crack growth was observed to occur. The cohesive law for these elements was identical to that established for quasi-static fracture in the previous section. In the absence of any mechanistic understanding of the transition to the brittle mode of fracture, these "tough" elements were placed along the interface over a length corresponding to the

experimentally observed initial extent of quasi-static crack growth. The rest of the interface (to the end of the specimen) was modeled with "brittle" elements. As discussed in the previous section, the tensile tests showed no rate sensitivity of the cohesive strength up to very large strain rates. Therefore, it was assumed that the cohesive strength was essentially identical for both dynamic fracture and quasi-static fracture. The brittle elements were set to have a cohesive strength of $24 \pm 3$ MPa, but an unknown toughness. The traction-separation laws corresponding to the two modes of fracture are shown in Fig. 7.

The numerical simulation was implemented using an ABAQUS 2-D implicit dynamic code, with the density of the steel set to 7800 kg/m$^3$. The crack initially grew in a quasi-static fashion through the initial region of tough elements, until it reached the region in which the brittle elements were placed. At that point it jumped in a dynamic fashion to a location within this second set of elements. The crack then began to grow in a quasi-static fashion again, but at a rate corresponding to the lower toughness. Reducing the toughness of the brittle elements resulted in a longer region of dynamic crack growth. Increasing the toughness resulted in a shorter region of dynamic crack growth. By matching the length over which unstable crack growth occurs to the length of the first jump in the experiments, the toughness of the brittle mode was determined to be $1.05 \pm 0.05$ kJ$\cdot$m$^{-2}$. This value of toughness consistently permitted the extent of the brittle fracture (and, hence, the return to the toughened mode of fracture) to be calculated correctly for different tests that exhibited transitions in the failure mode.

One possible concern with these calculations might be whether dynamic crack growth induces sufficiently large strain rates to violate the assumptions of rate-

independent plasticity in the numerical calculations. In fact, the calculations indicated that the dynamic portion of crack growth was accompanied only by elastic deformation of the adherends; plasticity only occurred after the much slower quasi-static crack growth had begun again. This would imply that any possible elevation of the yield stress associated with very high strain rates has no influence on the calculations (nor, on the transition mechanism). Validation that the numerical calculations were correctly capturing the deformation of the adherends during the dynamic phase of crack growth was obtained by calculating the behavior of the specimens *after* the initial period of dynamic fracture.

The behavior of specimens after the onset of dynamic fracture was examined by another series of calculations in which the tough and brittle elements were placed along the interface to verify (i) that the load-displacement curves during the quasi-static portions of crack growth could be accurately predicted, and (ii) that the extent of subsequent portions of dynamic fracture could be accurately predicted. Both sets of numerical calculations are sensitive to the values of the cohesive parameters and to the calculated deformations of the specimens (which also depend on the cohesive parameters). It should be emphasized that the only "fits" in these calculations are the points at which transition to the brittle mode of fracture occur - everything else in the model was fixed after the cohesive parameters had been determined. Examples of the results for the load-displacement curve and the crack lengths are shown in Figs. 8 and 9. It will be seen that the predictive portions of the numerical calculations are in excellent agreement with the experimental results. This implies that all the cohesive parameters are appropriate and reasonably uniform along the interface of a given specimen, and that

the deformation of the adherends was correctly modeled (*i.e*., dynamic effects on the constitutive properties of the adherends could be ignored).

## 5. Wedge Tests

The wedge tests described in the companion paper (Sun *et. al.*, 2008) provide a third mode-I geometry. For the purposes of this present paper, the results of these tests serve two distinct purposes. At lower loading rates, when the quasi-static crack velocities are comparable to the crack velocities obtained from the DCB tests, the wedge test provides an independent geometry that can be used to verify the cohesive parameters obtained by the other tests. As will be discussed later, the wedge test has characteristics that are sensitive to both the cohesive strength and the toughness; this makes it a useful independent geometry for validating the cohesive-zone parameters. The wedge test has a second advantage in that it can readily be loaded by a weight dropped under impact conditions, with much higher loading rates than can be obtained using the DCB geometry. There are four characteristic measurements that can be obtained from a wedge test with plastically deforming arms: (i) the curvature of the arms (Thouless *et al.* 1998; Yang *et al.*, 1999; Ferracin *et al.*, 2003); (ii) the extension of the crack ahead of the wedge (Ferracin *et al.*, 2003); (iii) the applied load (ISO 11343, 2003; Blackman *et al.*, 2000); and (iv) the total energy dissipated during the test (ISO 11343, 2003; Blackman *et al.*, 2000). These are discussed in the following sections.

### *5.1 Crack extension and curvature*

A static ABAQUS/Standard 2D model with cohesive elements along the interface was established to study the wedge tests. Owing to the symmetry of the geometry, only half the specimen was simulated (Fig. 10). The calculations were performed by forcing a

wedge along the interface between the adherends. The surfaces of the wedge and adherends were defined as contact surfaces. The geometry of the wedge and the specimens were based on the actual geometries used in the experiments of the companion paper, with one important exception: the thickness of the wedge was increased by an amount equal to the thickness of the adhesive layer. This correction was made because, while the intact cohesive elements had a thickness equal to that of the adhesive layer that they replaced, the numerical formulation resulted in the failed elements allowing direct contact with the steel surface. Adjusting the thickness of the wedge was chosen as the easiest method to compensate for this effect. Other approaches, such as explicitly incorporating an adhesive layer, or providing a finite thickness for the failed elements, could also have been adopted to accommodate the thickness of the adhesive behind the crack tip. In the present study, the properties of the cohesive elements corresponded, without modification, to what had been established from the other two tests. Both the crack extension ahead of the wedge, and the radius of the deformed arms were measured from the numerical mesh. These were then compared directly to the experimental results of Sun *et al.* (2008).

There were two main sources of uncertainty in the numerical predictions. One was associated with the range of uncertainty in the cohesive parameters. The other was associated with the fact that the fracture surface was not always smooth, as the crack sometimes oscillated within the adhesive layer. It was recognized that this effect could increase the effective thickness of the adhesive layer transmitting the load between the wedge and adherends. The uncertainty associated with this was included in the numerical calculations by investigating the effect of further thickening the wedge by about 0.5 mm,

equivalent to a substantial fraction of the thickness of the adhesive layer. Both of these uncertainties are reflected in the predictions of the numerical model that are presented below.

The experiments that exhibited quasi-static crack growth were modeled using the tough ($\Gamma_I = 4.2 \pm 0.3$ kJ/m$^2$) cohesive elements along the entire interface. The residual curvature of the deformed numerical mesh after fracture was found to be in the range of 7 to 13 m$^{-1}$. This is consistent with the experimental values of $10 \pm 2$ m$^{-1}$ quoted in the companion paper for the quasi-static tests. The calculated distance between the crack tip and the wedge fell in the range of 6 to 9 mm. This, again, is consistent with the observed range of 5 to 9 mm for all quasi-static crack velocities, as described in the companion paper.

The details of the contact between the wedge and adherends depend on the deformation history of the specimen. Therefore, in the absence of a mechanistic model for the transition to brittle fracture, *a priori* analyses of the specimens that exhibit the transition are limited to providing bounds for the predicted behavior. Although steady-state brittle behavior was never observed experimentally, a calculation in which brittle elements are placed along the entire interface provides a limiting calculation that would be an approximation for the fastest rates of loading, in which transitions to brittle fracture were extremely likely. The numerical curvature measured from the deformed mesh after fracture with brittle elements along the entire interface was in the range of 0.6 to 1.4 m$^{-1}$; this provides a lower bound to the experimental observations of $2.0 \pm 0.2$ m$^{-1}$ for the curvature at the fastest wedge velocities, which exhibited quasi-static crack growth over regions of up to 10% of the bonded interface. These numerical calculations also

indicated that the crack tip advanced about 15 ± 2 mm ahead of the wedge for a model with a completely brittle interface; this is consistent with the upper end of the experimental observations for all rates of loading. A second limit was provided by a calculation in which tough elements were placed over the first 20 mm of the interface, to allow steady-state quasi-static crack growth to be established, followed by brittle elements over the rest of the interface. The results of these calculations indicated that when the crack made the transition from quasi-static crack growth at the boundary between the two sets of elements, it jumped forward and arrested 10 mm ahead of the wedge. These results were consistent with the lower range of the experimental observations for the crack length associated with the arrest of dynamic fracture.

These numerical predictions were produced with no input from the experimental observations, and with the *caveat* that we currently have no mechanistic model for the statistical transitions to brittle failure. Thus, the good agreement between the predictions and the experimental observations provide some level of independent validation for the values of the cohesive parameters obtained in the first section of the paper. In addition, the results of the wedge tests support the conclusion that, for this system, the cohesive parameters for quasi-static crack growth in the toughened mode are essentially independent of crack velocity, even up to crack velocities at least as high as 1000 mm/s.

*5.2 Energy dissipation and the effects of friction*

A recent ISO standard (ISO 11343, 2003) proposes that a wedge test may be used to characterize fracture by measuring the load on the wedge and the energy dissipated when the wedge is moved through the bond. Such a test introduces an obvious concern about the effects of friction on these measurements. The frictional force between the

wedge and the adherend is oriented in such a direction that it makes a minimal contribution to fracture, but is expected to be a major contribution of any force parallel to the interface that might be measured in such a test. Furthermore, it seems possible that a major portion of the energy dissipated during fracture by a wedge may be attributed to friction. In an analysis of the ISO wedge test, Blackman *et al.* (2000) provided numerical calculations indicating that an increase in the coefficient of friction from 0 to 0.5 might increase the applied force by no more than 20%, and that frictional effects can be ignored in the wedge test. A simple calculation suggests that this conclusion is unlikely to be generally valid. Consider a wedge with a half angle of θ that makes contact with the specimen at a single point on each arm. If there is no friction, only a normal force acts at the contact and provides a bending moment (and transverse shear force) that act at the crack tip to propagate the crack. If the critical magnitude of this normal force is $N_f$, then the applied force required to move the wedge through the bond is

$$P_f = 2N_f \sin\theta \ . \qquad (1)$$

If it is assumed that the critical normal force required to propagate the crack does not change with friction, then the applied force required to move the wedge through the bond becomes

$$P_f = 2N_f\left(\sin\theta + \mu\cos\theta\right) \qquad , \qquad (2)$$

when the coefficient of friction is μ. A typical half-wedge angle in these tests is about 5º; so, these equations suggest that frictional effects will increase the applied load (and energy) by a factor of about 6.7 with μ = 0.5. Since these calculations indicate that friction may dominate the energy dissipation in a wedge test, the numerical calculations were extended to examine this issue.

The effect of friction during quasi-static crack growth was considered by using a 2-D static cohesive-zone model, as described in the previous section, and comparing the results with two different experimental observations: (i) the energy dissipated during quasi-static fracture in a drop-tower experiment, and (ii) the reaction load measured during the quasi-static tests conducted in the mechanical testing machine. In the numerical calculations, tough elements ($\Gamma_I = 4.2 \pm 0.3$ kJ/m$^2$) were placed all along the interface, and Coulomb friction was assumed between the wedge and the adherends. The energy associated with separation of the interface, plastic deformation, elastic deformation, and friction were all evaluated separately, as was the reaction force on the wedge. The results showed that, in addition to $4.2 \pm 0.3$ kJ/m$^2$ of cohesive energy being dissipated, an additional $2.7 \pm 0.5$ kJ/m$^2$ was dissipated by the plastic deformation of the adherends. In the absence of friction, the reaction force on the wedge was about 150 N. The presence of friction had a profound effect on the reaction force, but did not significantly affect either the curvature of the arms or the propagation of the crack.

The companion paper (Sun *et al.*, 2008) reported that in one drop-tower test with a mass of 40 kg and coupons that were 20 mm wide, the mass was brought to rest after it had traveled 95.5 mm and the crack had propagated 30 mm in a quasi-static fashion. The potential energy lost by the mass in this experiment was 37.5 J. The results of the numerical calculations indicate that only $4.1 \pm 0.5$ J (cohesive energy plus plasticity) is directly associated with 30 mm of quasi-static crack growth. Therefore, $33.4 \pm 0.5$ J must have been dissipated by friction, before, and during, crack propagation. By adjusting the coefficient of friction in the numerical model, this energy dissipation could be matched if the coefficient of friction was set to $0.32 \pm 0.02$. The numerical results are summarized

in Fig. 11, which shows how the elastic energy stored, the plastic energy dissipated, the fracture energy dissipated, and the frictional energy dissipated all vary with wedge displacement for a quasi-static test. The reaction force on the wedge (parallel to the interface) was computed to be about 600 N with $\mu = 0.32$, which was in excellent agreement with the loads measured for the quasi-static wedge tests done in the mechanical testing machine at different rates. This is illustrated in the plot of Fig. 12 that shows a comparison between the numerical calculations of the reaction force and the measured values. Furthermore, the increase by a factor of four in the applied load, associated with increasing the friction coefficient from 0 to 0.32, is consistent with the increase predicted by Eqn. 2.

Transitions to a brittle-mode of fracture result in lower wedge loads, and in lower levels of energy dissipation dissipated. Therefore, as a point of comparison, similar calculations were also done with brittle cohesive elements. For the particular set of materials used in this study, the plastic dissipation associated with brittle fracture was calculated to be $0.2 \pm 0.1$ kJ/m$^2$, compared to a cohesive energy of $1.05 \pm 0.05$ kJ/m$^2$. Crack growth with alternating regimes of toughened and brittle failure modes is more complicated, since, dynamic fracture occurs without movement of the wedge and is, therefore, divorced from frictional considerations, except as the wedge moves to catch up with the new crack position to begin quasi-static crack growth again. Furthermore, plastic deformation of the arms does not actually occur during the dynamic, brittle portion of the crack growth - it only occurs as the wedge advances to initiate quasi-static crack growth again.

In summary, for quasi-static fracture with the wedge geometry and materials used in this study: 13% of the energy is dissipated by fracture of the adhesive layer, 9% is dissipated by the accompanying plastic deformation, and the remaining 78% is dissipated by friction. Clearly, the implication of these calculations is that the force and energy are dominated by frictional effects, and would not have been suitable quantities to use in an attempt to determine quantitative values of the cohesive parameters.

*5.3 Use of the wedge test to determine cohesive parameters*

In this paper, the results of the wedge test have been used primarily to verify the cohesive parameters obtained from other tests, in addition to exploring the effects of higher loading rates. However, it would also have been possible to use the wedge tests to determine the cohesive parameters directly. As discussed above, the effects of friction are probably too great to make measurements of the load and energy dissipated useful in anything approaching a quantitative fashion. However, both the residual curvature of plastically deforming arms (Yang *et al.*, 1999) and the crack extension ahead of the wedge (Ferracin *et al.*, 2003) can be used quantitatively. In general, the two cohesive parameters have to be determined from at least two independent tests. Yang *et al.* (1999) demonstrated how to use the radii of curvature obtained using different thicknesses of wedges to determine the cohesive properties of an adhesive bonding aluminum. In a numerical paper Ferracin *et al.* (2003) analyzed this approach and, additionally, suggested the possibility of measuring both the curvature and crack length from a single test. Using this latter approach, the experimental results presented in the companion paper can be used to deduce the cohesive parameters, as shown in Fig. 13.

Figure 13 shows the regimes of toughness and strength pairs that would provide numerical fits to the experimental observations of the residual curvature and crack extension given in Sun *et al.* (2008). As can be seen from this figure, the crack length (for this particular system) is insensitive to the cohesive strength, while the curvature has a dependence on both cohesive parameters. A comparison between Fig. 3 and Fig. 13 will show that the bounds imposed on the values of the cohesive parameters by the results of the wedge test are consistent with the bounds imposed by the DCB and tensile tests. However, the details of the results from the wedge test are very sensitive to the details of the system. Therefore, the uncertainties in the values of the parameters would have been somewhat larger had they been determined from the wedge test, rather than from the process actually used in this paper. However, this discussion emphasizes that the wedge test does provide a third and independent configuration that can be used as validation of the cohesive parameters.

**6. Conclusions**

A transition between quasi-static and dynamic crack growth is responsible for "stick-slip" behavior observed in Sun *et al.* (2008). The crack grew either in a quasi-static fashion at a rate determined by the geometry, loading rate and the material and cohesive properties, or it propagated in an unstable, dynamic fashion. The toughness in both regimes can be determined by comparing numerical predictions to experimental observations of double-cantilever-beam (DCB) tests. For the particular combination of materials investigated in this project, the DCB geometry is not very sensitive to the cohesive strength of the interface. Therefore, an alternative tensile test was developed to determine the cohesive strength. The toughened and brittle cohesive parameters were

verified by performing numerical calculations for a wedge geometry, and comparing the predictions to the test data. Furthermore, the numerical calculations allowed the effects of friction to be determined. It was shown that in the wedge experiments conducted in this study, the cohesive energy can account for as little as 13% of the total energy dissipated, with friction accounting for as much as 78%. As a result, measurements of the load or work required to split the wedge would not have provided useful measures of the cohesive properties of the joint. However, simultaneous measurements of the curvature and crack extension could have provided values of the cohesive parameters (albeit, with more uncertainty than the approach chosen).

The cohesive parameters for the quasi-static mode of crack growth appeared to be essentially independent of rate. Catastrophic transitions to the brittle mode occurred randomly, but with an increased frequency at higher crack velocities. These observations make some connection to observations of rate effects in rubber-toughened epoxies by Du *et al*. (2000), which suggested that the toughening mechanisms of cavitation and void growth were rate independent, and the onset of dynamic fracture was associated with a catastrophic switching off of the toughening mechanism.[5] While a unified model for transitions in the crack growth behavior has not been elucidated, several features that would be required of such a model have emerged from the analysis in this paper and the observations in the companion paper. In particular, some of the simpler approaches that might be adopted to model the ductile-brittle transition in this system with a toughened

[5] Interpretation of the results of Du *et al.* (2000) is complicated because of *R*-curve effects in which the process zone increases with the applied energy-release rate. In the present case of an adhesive bond, the width of the process zone is limited by the bond thickness. The relatively narrow range that was obtained for the toughness in this study, supports the notion that the process zone quickly extends to the full width of the bond.

adhesive system are not appropriate. For example, the absence of rate-dependent cohesive parameters rules out models that rely on stable and unstable branches of the velocity-toughness curve. Equally, a model where one of the cohesive parameters (such as the strength associated with triggering the toughening mechanism) increases with crack velocity, until it exceeds the value associated with brittle fracture (such as a cleavage strength) can't be complete, because quasi-static crack growth occurred at velocities vastly in excess of the lowest velocities at which the transition was seen. However, it might be possible to develop a model based on this concept provided an element of probability was introduced.

A model that might be consistent with the experimental observations, could have the two rate-independent cohesive laws used in this study, but would have to incorporate a range of uncertainty in the strength for the toughened law. The cleavage strength and the range of strengths to trigger the toughening mechanism would have to be very comparable (within the experimental uncertainty of this paper), as proposed in the models used in the earlier sections. Once an element started to move along either unloading trajectory, it would have to follow that trajectory until final failure of the element. (This could mean, for example, that once cavitation had been induced brittle cleavage could not occur in that element of material.) The model could accommodate the statistical nature of the problem by introducing a rate-dependent probability for choosing the unloading portion of the traction-separation law. As an example of a model that might work with extensive tuning, one might explore the possibility that the toughening mechanism will be triggered at any point during loading according to a Weibull probability such as

$$P_t = 1 - \exp\left(-\frac{t}{t_o}\left(\frac{\sigma}{S_o}\right)^m\right), \qquad (3)$$

where σ is the traction on the element, $t$ is the time interval over which the element experiences the traction, $S_o$ is a characteristic strength associated with the toughening mechanism, ($t_o$ is chosen for non-dimensionalization purposes, and would depend on $S_o$), and $m$ controls the sensitivity of the probability to the stress. In particular, the experimental evidence suggests that $m$ would have to be very high to limit the practical changes in probability to the observed range of uncertainty in the strength. The cleavage strength associated with the brittle mechanism of crack growth would also need to be in this range. If an element continued loading until it reached this value of cohesive strength, without the toughening mechanism being triggered, then the element would follow the brittle law upon unloading. Conversely, if the toughening mechanism was triggered, then the element would follow the toughened law upon unloading. Variations on this type of model could equally well be explored; for example, one might try linking the probability of triggering the ductile-brittle transition to the current quasi-static crack velocity.

Although an outline of a potential numerical model for the transition has been given to provide a possible physical understanding of the transition mechanism, a statistical approach may be an inappropriate design approach for energy absorption in crashes. In this regard, the strategy adopted in this paper, determining the cohesive properties for both mechanisms, provides a tool for furnishing upper and lower bound descriptions of the behavior, corresponding to quasi-static crack growth and a most-brittle-case scenario. These can be used for numerical predictions of energy absorption

during impact loading of adhesive joints, since the ratio of change in energy dissipated by plasticity to energy dissipated in the adhesive layer is very sensitive to the cohesive properties of the adhesive layer and the properties of the adherends. Cohesive models of the sort discussed in this paper are expected to be of great utility for designing and optimizing joints for energy management during impact.

**Acknowledgements**

C. Sun, M. D. Thouless and A. M. Waas gratefully acknowledge the financial support of General Motors.

**References**


Alfano, G. "On the influence of the shape of the interface law on the application of cohesive-zone models," *Composites Science and Technology*, **66**, 723-730 (2006)

Andersson, T. and Stigh, U. "The stress-elongation relation for an adhesive layer loaded in peel using equilibrium of energetic forces," *International Journal of Solids and Structures*, **41**, 413-434 (2004).

Andersson, T. and Biehl, A. "On the effective constitutive properties of a thin adhesive layer loaded in peel," *International Journal of Fracture*, **141**, 227-246 (2006).

Blackman, B. R. K., Kinloch, A. J., Taylor, A. C. and Wang, Y. "The impact wedge-peel performance of structural adhesives," *Journal of Materials Science*, **35** 1867-1884 (2000).

Cavalli, M. N. and Thouless, M. D. " The effect of damage nucleation on the toughness of an adhesive joint," *Journal of Adhesion,* **76**, 75-92. (2001).

Chandra, N., Li, H., Shet, C. and H. Ghonem, H. "Some issues in the application of cohesive zone models for metal–ceramic interface," *International Journal of Solids and Structures*, **39**, 2827-2855 (2002).

Du, J, Thouless, M. D. and Yee, A. F. "Effects of rate on crack growth in a rubber-modified epoxy," *Acta Materialia*, **48**, 3581-3592 (2000).

Ferracin, T., Landis, C. M., Delannay, F. and Pardoen, T. "On the determination of the cohesive zone properties of an adhesive layer from the analysis of the wedge-peel test." *International Journal of Solids and Structures*, **40**, 2889-2904 (2003).

ISO 11343 (2003) "Adhesives - Determination of dynamic resistance to cleavage of high-strength adhesive bonds under impact conditions - wedge impact method"

Kubair, D. V., Geubelle, P. H. and Huang, Y. Y. "Analysis of a rate-dependent cohesive model for dynamic crack propagation," *Engineering Fracture Mechanics*, **70**, 685-704 (2005).

Landis, C. M., Pardoen, T. and Hutchinson, J. W. "Crack velocity dependent toughness in rate dependent materials," *Mechanics of Materials*, **32**, 663-678 (2000).

Li, V. C., Chan, C. M. and Leung, C. K. Y. "Experimental determination of the tension-softening relations for cementitious composites," *Cement and Concrete Research,* **17**, 441–52 (1987).

Li, H. and Chandra, N. "Analysis of crack growth and crack-tip plasticity in ductile materials using cohesive zone models," *International Journal of Plasticity*, **19**, 849-882 (2003).

Li S., Thouless, M. D., Waas, A. M., Schroeder, J. A. and Zavattieri, P. D. "Use of mode-I cohesive-zone models to describe the fracture of an adhesively-bonded polymer-matrix composite," *Composites Science and Technology*, **65** (2), 281-293 (2005a)

Li S., Thouless, M. D., Waas, A. M., Schroeder, J. A. and Zavattieri, P. D. "Use of a cohesive-zone model to analyze the fracture of a fiber-reinforced polymer–matrix composite," *Composites Science and Technology*, **65**, 537-549 (2005b).

Madhusudhana, K. S. and Narasimhan, R. "Experimental and numerical investigations of mixed-mode crack growth resistance of a ductile adhesive joint," *Engineering Fracture Mechanics*, **69**, 865-883 (2002)

Maugis, D. "Review subcritical crack growth, surface energy, fracture toughness, stick-slip and embrittlement," *Journal of Materials Science*, **20**, 3041-3073(1985).

Rahulkumar, P., Jagota, A., Bennison, S. J. and Saigal, S. "Cohesive element modeling of viscoeleastic fracture: application to peel testing of polymers," *International Journal of Solids and Structures,* **37**, 1873-1897 (2000).

Sørensen, B. F. "Cohesive law and notch sensitivity of adhesive joints," *Acta Materialia*, **50**, 1053–61 (2002).

Sørensen, B. F. and Jacobsen T. K. "Determination of cohesive laws by the *J* integral approach," *Engineering Fracture Mechanics,* **70,** 1841–185 (2003).

Su, C., Wei, Y. J. and Anand, L. "An elastic-plastic interface constitutive model: application to adhesive joints," *International Journal of Plasticity,* **20**, 2063-2081 (2004).

Sun C., Thouless M. D., Waas A. M., Schroeder J. A. and Zavattieri P. D. "Mode-I stick-slip fracture in plastically deforming, adhesively-bonded structures: I Experimental studies," *International Journal of Solids and Structures*, in press (2008).

Thouless, M. D., Kafkalidis, M. S., Adams, J. L., Ward, S. M., Dickie, R. A. and Westerbeek, G. L. "Determining the toughness of adhesives in plastically-deforming joints," *Journal of Materials Science*, **33**, 189-197 (1998).

Tvergaard, V. and Hutchinson, J. W. "Toughness of an interface along a thin ductile layer joining elastic solids," *Philosophical Magazine A*, **70**, 641-656 (1994)

Tvergaard, V. and Hutchinson, J. W. "On the toughness of ductile adhesive joints," *Journal of the Mechanics and Physics of Solids*, **44**, 789-800 (1996).

Ungsuwarungsri, T. and Knauss, W. G. "Role of damage-softened material behavior in the fracture of composites and adhesives," *International Journal of Fracture*, **35**, 221–41 (1987).

Williams, J. G. *Fracture Mechanics of Polymers*, Ellis Horwood Limited, Chichester, UK (1984).

Yang, Q. D., Thouless, M. D. and Ward, S. M. (1999). "Numerical simulations of adhesively bonded beams failing with extensive plastic deformation," *Journal of the Mechanics and Physics of Solids*, **47**, 1337–1353.

Yang, Q. D. and Thouless, M. D. "Mixed-mode fracture analyses of plastically-deforming adhesive joints," *International Journal of Fracture,* **110,** 175-187 (2001).

Zhou, F. Molinari J.-F. and Shioya, T. "A rate-dependent cohesive model for simulating dynamic crack propagation in brittle materials," *Engineering Fracture Mechanics*, **72**, 1383-1410 (2005).

**Figure Captions**

**Figure 1** An example of the trapezoidal mode-I traction-separation law used for quasi-static fracture of the adhesive layer.

**Figure 2** Configuration of the DCB geometry used for the numerical simulations.

**Figure 3** A plot showing the ranges of values for the mode-I toughness and normal cohesive strength values that give an acceptable agreement between the numerical and experimental results for the DCB geometry and tensile test geometry.

**Figure 4** Configuration of the tensile test specimen used to evaluate the cohesive strength of the adhesive system. Two steel coupons are bonded in the middle by the adhesive. These coupons are bonded to thick steel tabs that transmit the load.

**Figure 5** Fit between the DCB experimental load-displacement data and the numerical predictions of a cohesive-zone model, showing upper and lower bounds for the fit. The toughness for the adhesive was determined to be $4.2 \pm 0.3$ kJm$^{-2}$.

**Figure 6** Fit between the experimental crack length *versus* cross-head displacement data and the numerical predictions for quasi-static crack growth in the DCB geometry. The numerical predictions are based on a cohesive model with a mode-I toughness of $4.2 \pm 0.3$ kJm$^{-2}$ and a cohesive strength of $24 \pm 3$ MPa.

**Figure 7** A comparison between the two traction-separation laws used for quasi-static and for dynamic fracture. The cohesive strength, $\hat{\sigma}$, was fixed at $24 \pm 3$ MPa for both laws. The toughness for the "tough" (quasi-static)

elements was fixed at $4.2 \pm 0.3$ kJm$^{-2}$ The toughness for the "brittle" (dynamic) elements was found to be equal to $1.05 \pm 0.05$ kJm$^{-2}$.

**Figure 8** Fit between the experimental load-displacement data for the DCB specimens at a loading rate of 150 mm/s in which dynamic fracture occurred, and the numerical predictions of the two-part cohesive-zone model.

**Figure 9** Comparison between the experimental data for the variation in crack length with cross-head displacement and the numerical predictions from a cohesive-zone model for the DCB geometry in which dynamic fracture occurred at an applied displacement rate of 150 mm/s.

**Figure 10** A static ABAQUS/Standard 2D model was used to simulate the wedge tests. Owing to the symmetry of geometry, only half of the specimen was simulated. The calculation was performed by forcing the wedge along the interface between the steel coupons. Contact elements were placed along the surfaces of the wedge and adherends. This figure shows the curvature of the steel arm after fracture.

**Figure 11** The results of a numerical calculation for a quasi-static wedge test with a coefficient of friction equal to 0.32. The plots show how the elastic energy stored in the geometry, the plastic energy dissipated, the fracture energy dissipated and the frictional energy dissipated vary with wedge displacement.

**Figure 12** A comparison between the reaction load on the wedge computed for the quasi-static tests with a coefficient of friction equal to 0.32, and loads measured during quasi-static tests.

**Figure 13** A plot showing the ranges of values for the mode-I toughness and cohesive strength values that give an acceptable agreement between the results of numerical calculations, and the two experimental measurements that could be obtained from the wedge test.

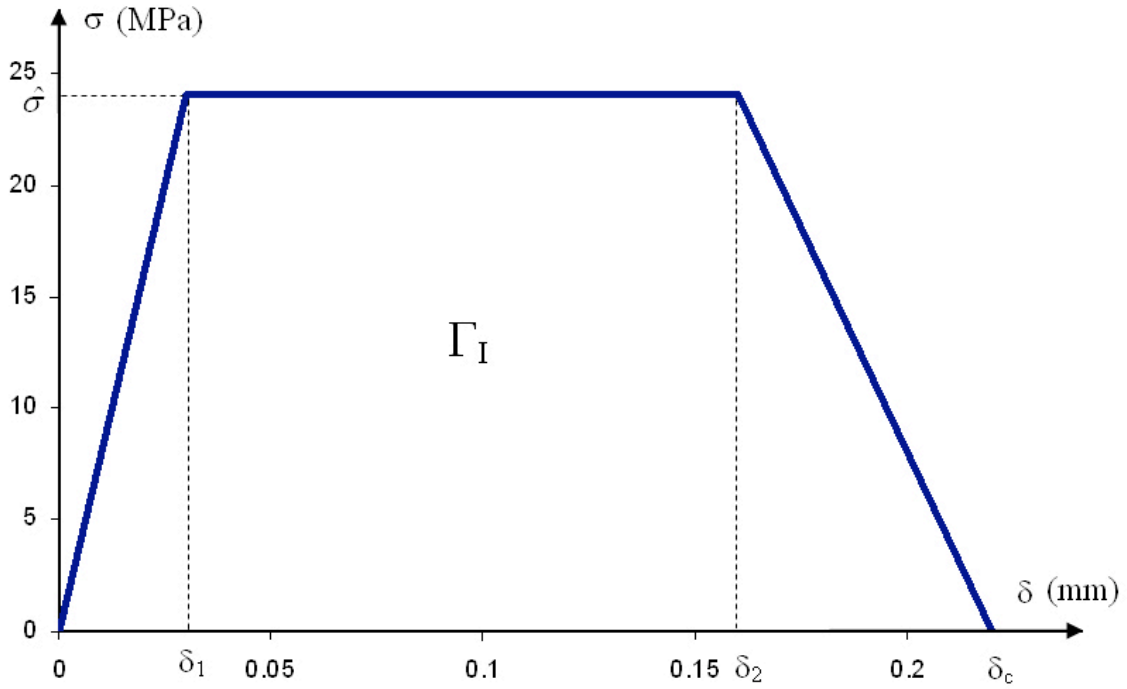


**Figure 1** An example of the trapezoidal mode-I traction-separation law used for quasi-static fracture of the adhesive layer.

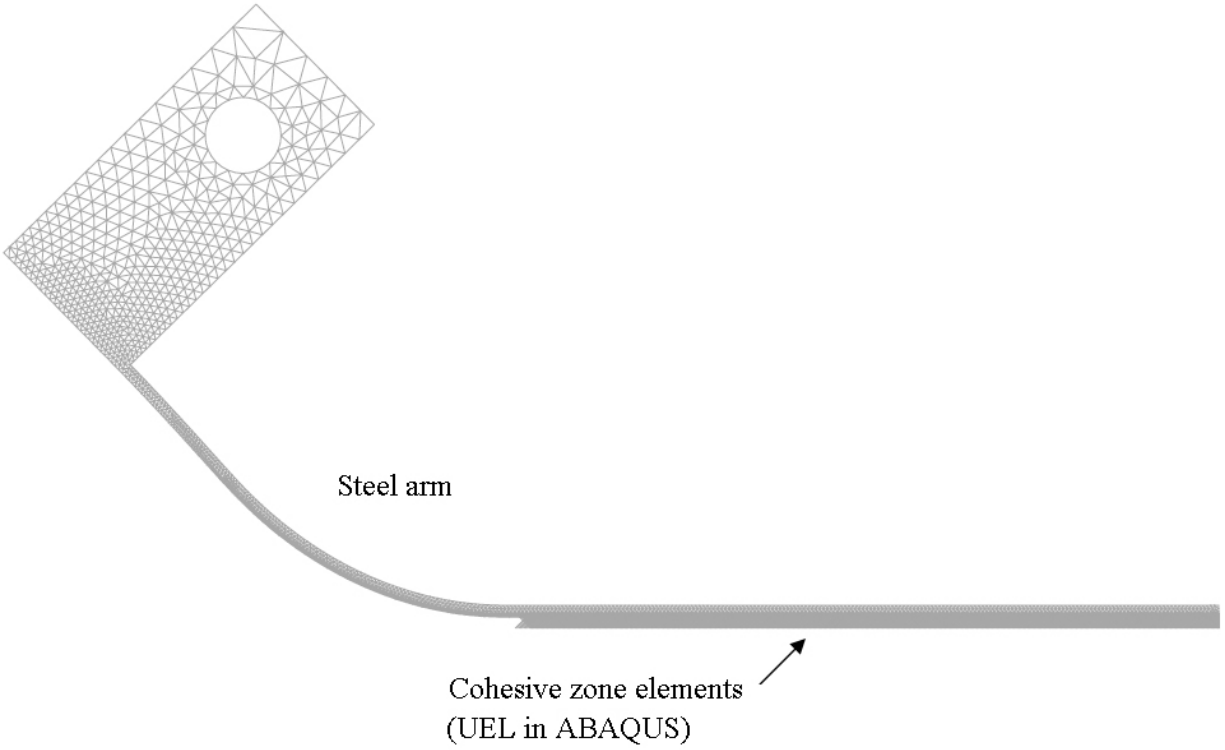


**Figure 2** Configuration of the DCB geometry used for the numerical simulations.

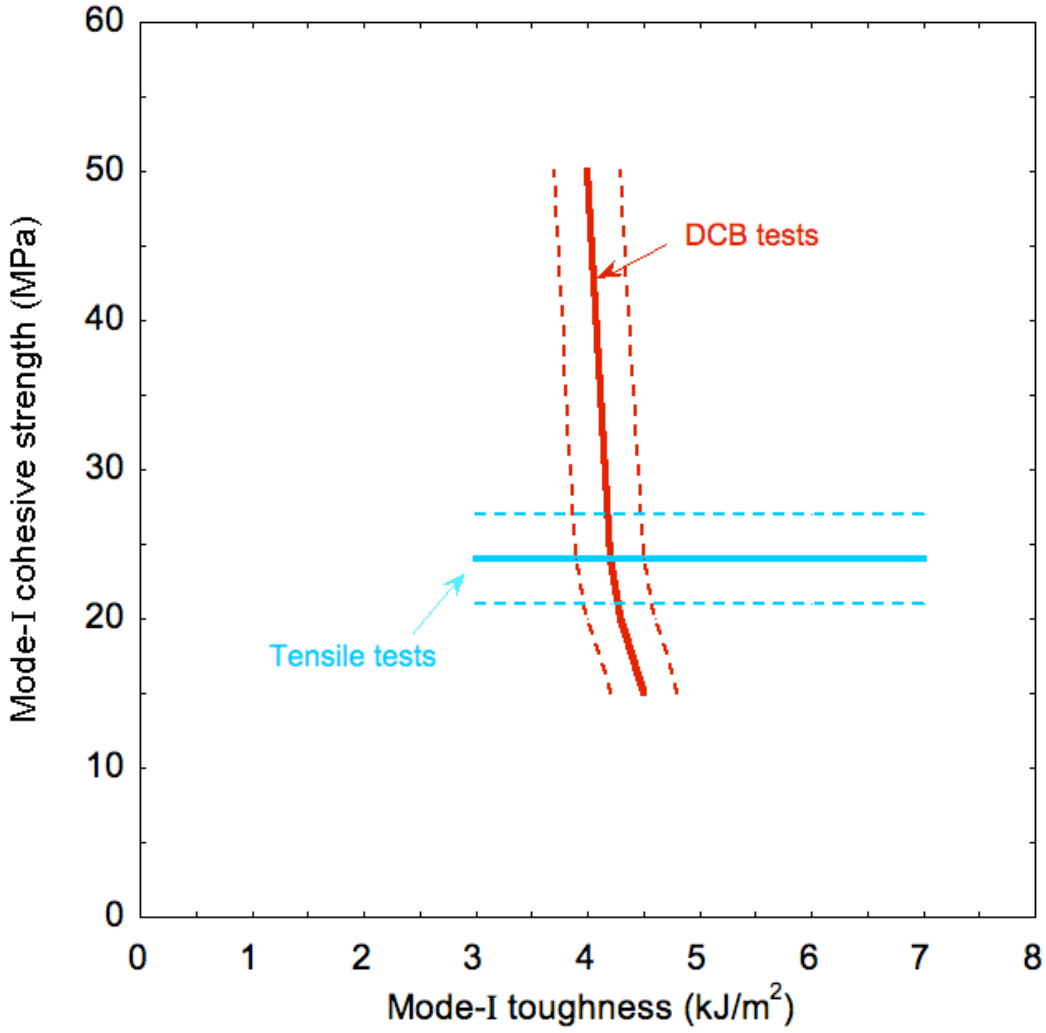


**Figure 3** A plot showing the ranges of values for the mode-I toughness and normal cohesive strength values that give an acceptable agreement between the numerical and experimental results for the DCB geometry and tensile test geometry.

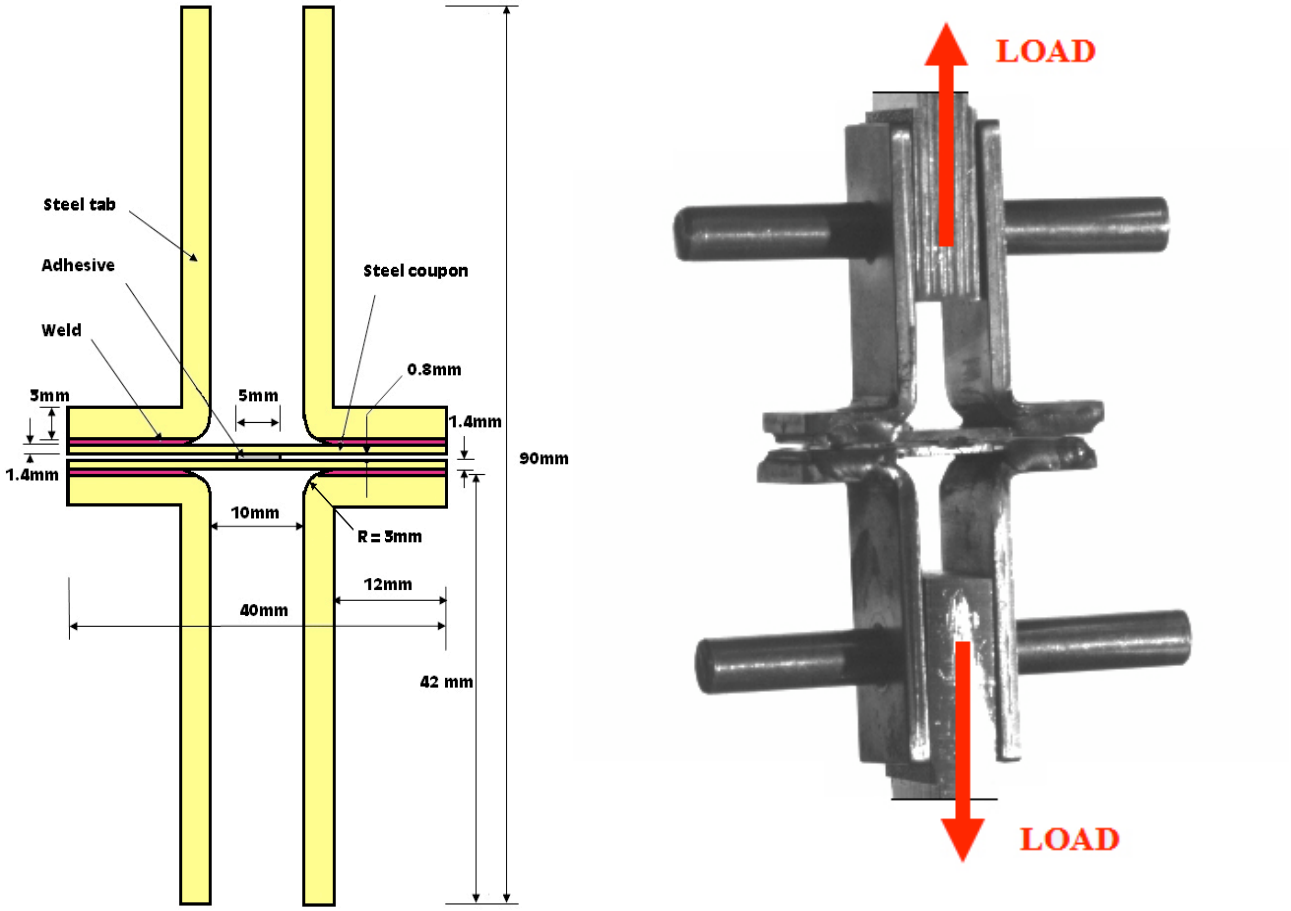


**Figure 4** Configuration of the tensile test specimen used to evaluate the cohesive strength of the adhesive system. Two steel coupons are bonded in the middle by the adhesive. These coupons are bonded to thick steel tabs that transmit the load.

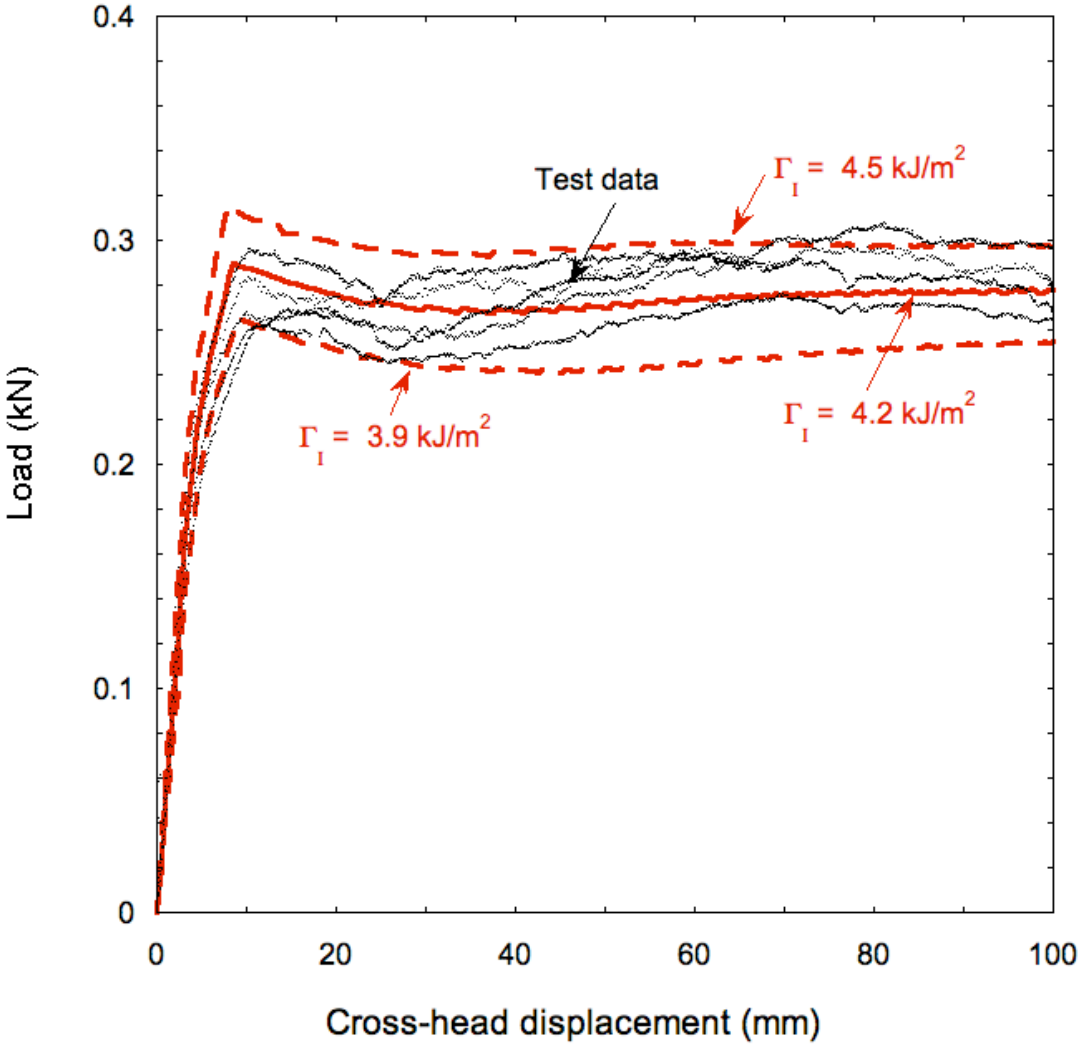


**Figure 5** Fit between the DCB experimental load-displacement data and the numerical predictions of a cohesive-zone model, showing upper and lower bounds for the fit. The toughness for the adhesive was determined to be $4.2 \pm 0.3$ kJm$^{-2}$.

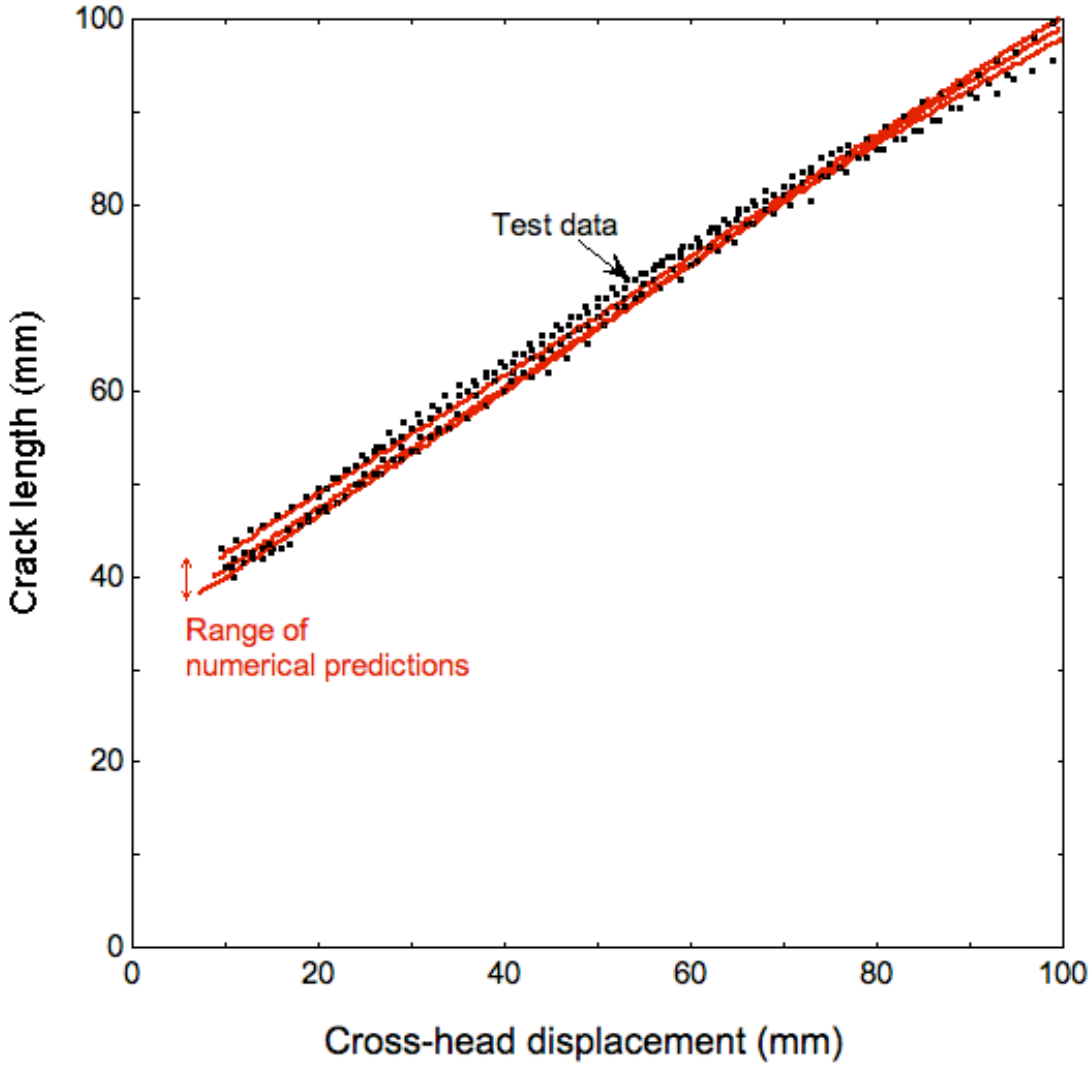


**Figure 6** Fit between the experimental crack length *versus* cross-head displacement data and the numerical predictions for quasi-static crack growth in the DCB geometry. The numerical predictions are based on a cohesive model with a mode-I toughness of $4.2 \pm 0.3$ kJm$^{-2}$ and a cohesive strength of $24 \pm 3$ MPa.

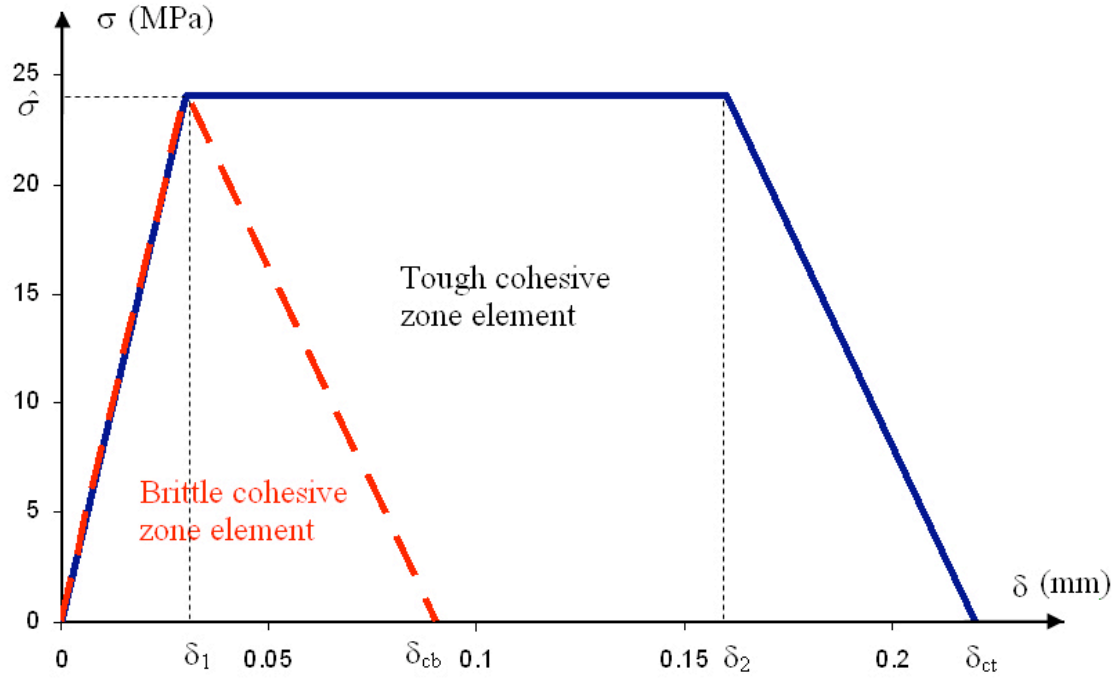


**Figure 7** A comparison between the two traction-separation laws used for quasi-static and for dynamic fracture. The cohesive strength, $\hat{\sigma}$, was fixed at $24 \pm 3$ MPa for both laws. The toughness for the "tough" (quasi-static) elements was fixed at $4.2 \pm 0.3$ kJm$^{-2}$ The toughness for the "brittle" (dynamic) elements was found to be equal to $1.05 \pm 0.05$ kJm$^{-2}$.

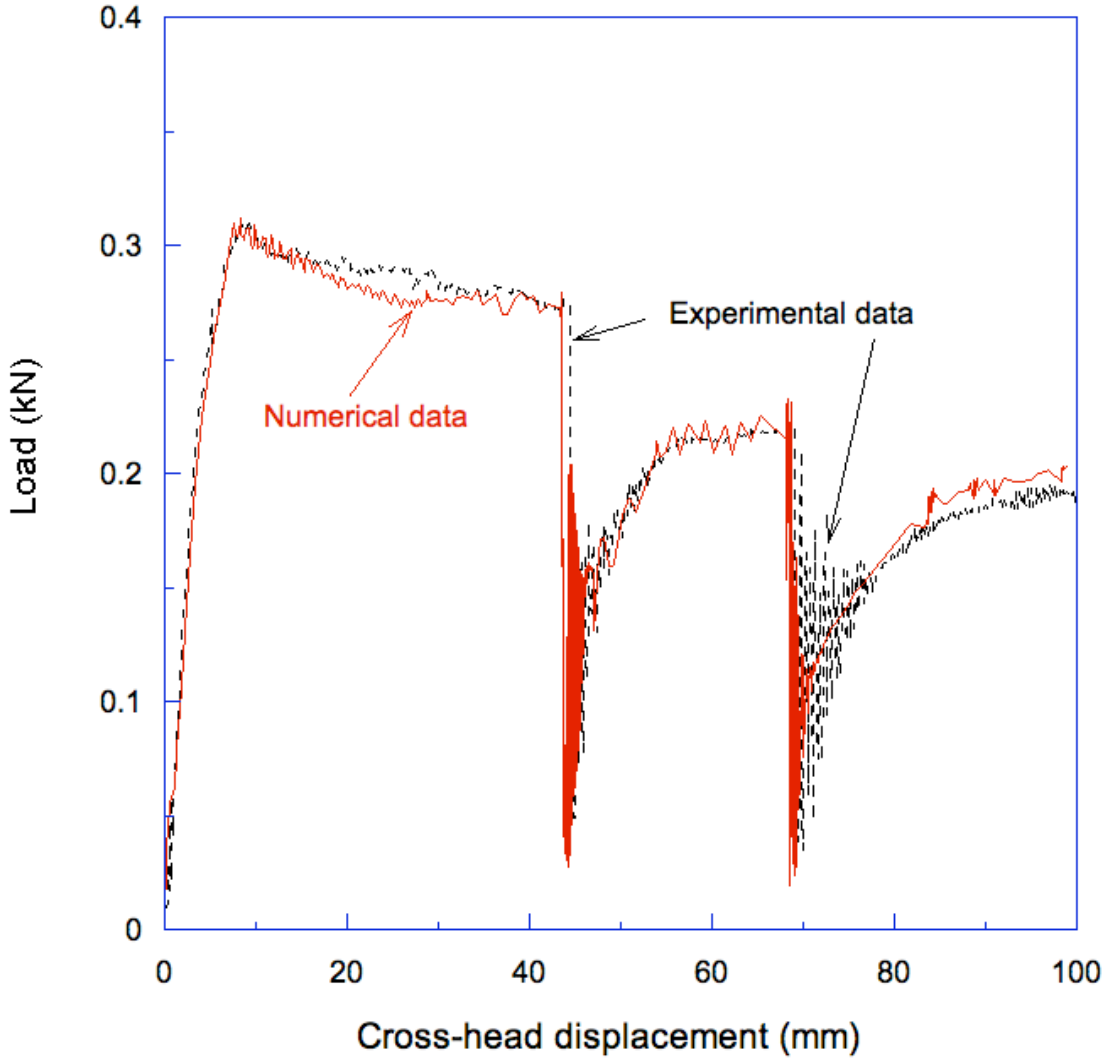


**Figure 8** Fit between the experimental load-displacement data for the DCB specimens at a loading rate of 150 mm/s in which dynamic fracture occurred, and the numerical predictions of the two-part cohesive-zone model.

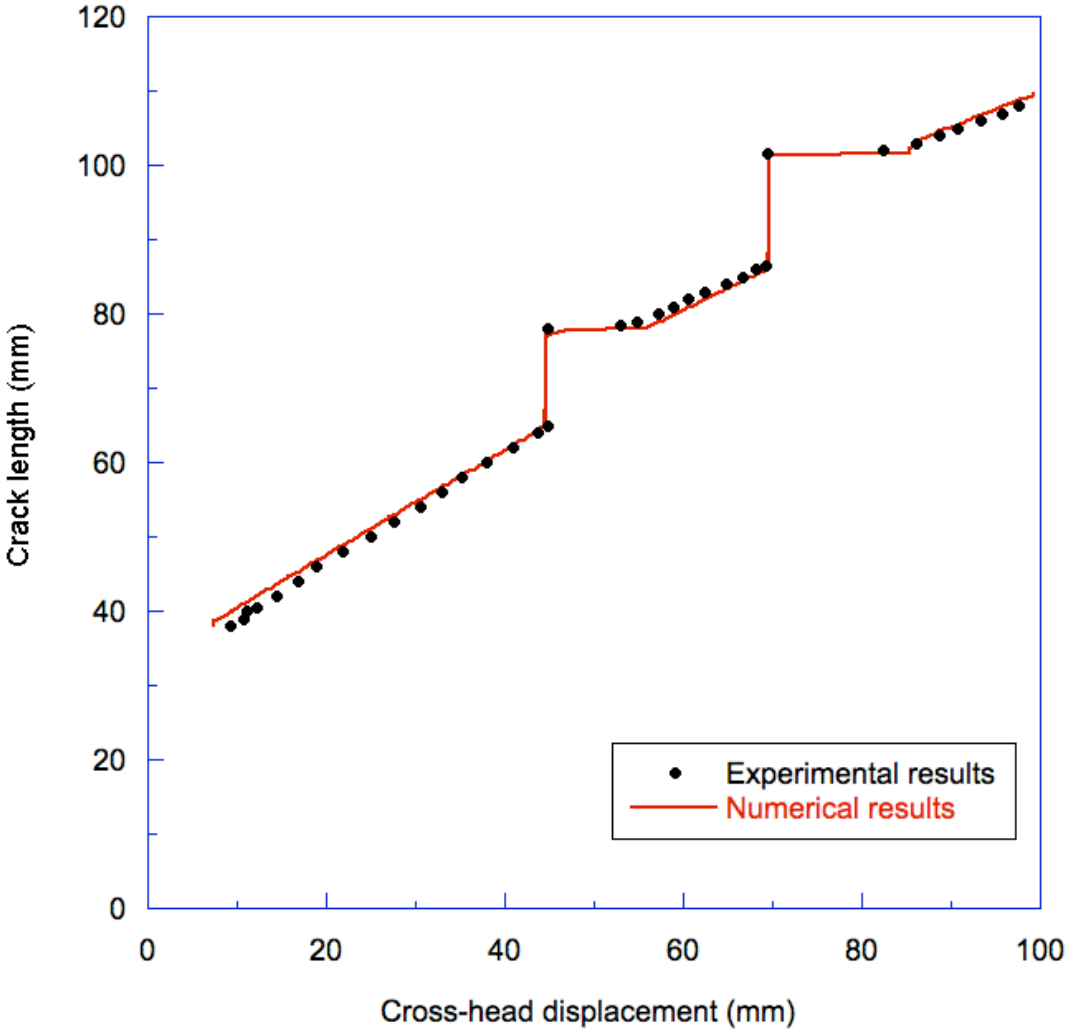


**Figure 9** Comparison between the experimental data for the variation in crack length with cross-head displacement and the numerical predictions from a cohesive-zone model for the DCB geometry in which dynamic fracture occurred at an applied displacement rate of 150 mm/s.

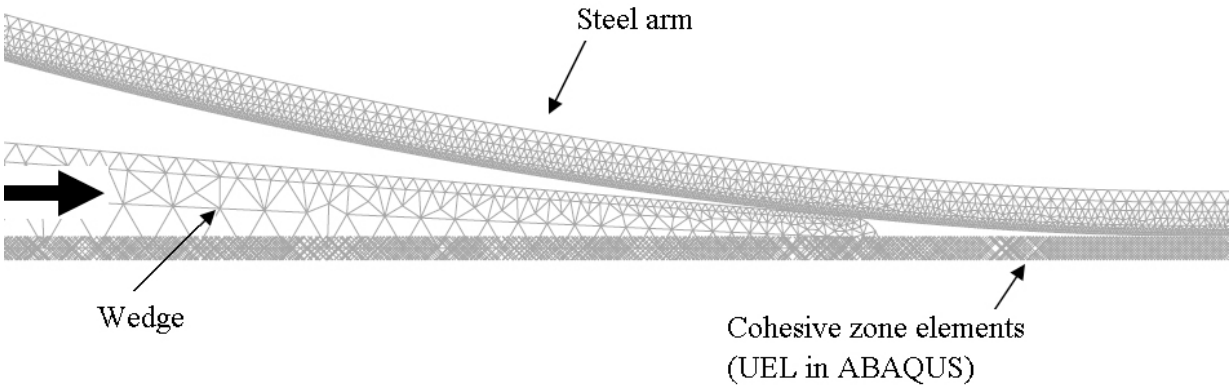


**Figure 10** A static ABAQUS/Standard 2D model was used to simulate the wedge tests. Owing to the symmetry of geometry, only half of the specimen was simulated. The calculation was performed by forcing the wedge along the interface between the steel coupons. Contact elements were placed along the surfaces of the wedge and adherends. This figure shows the curvature of the steel arm after fracture.

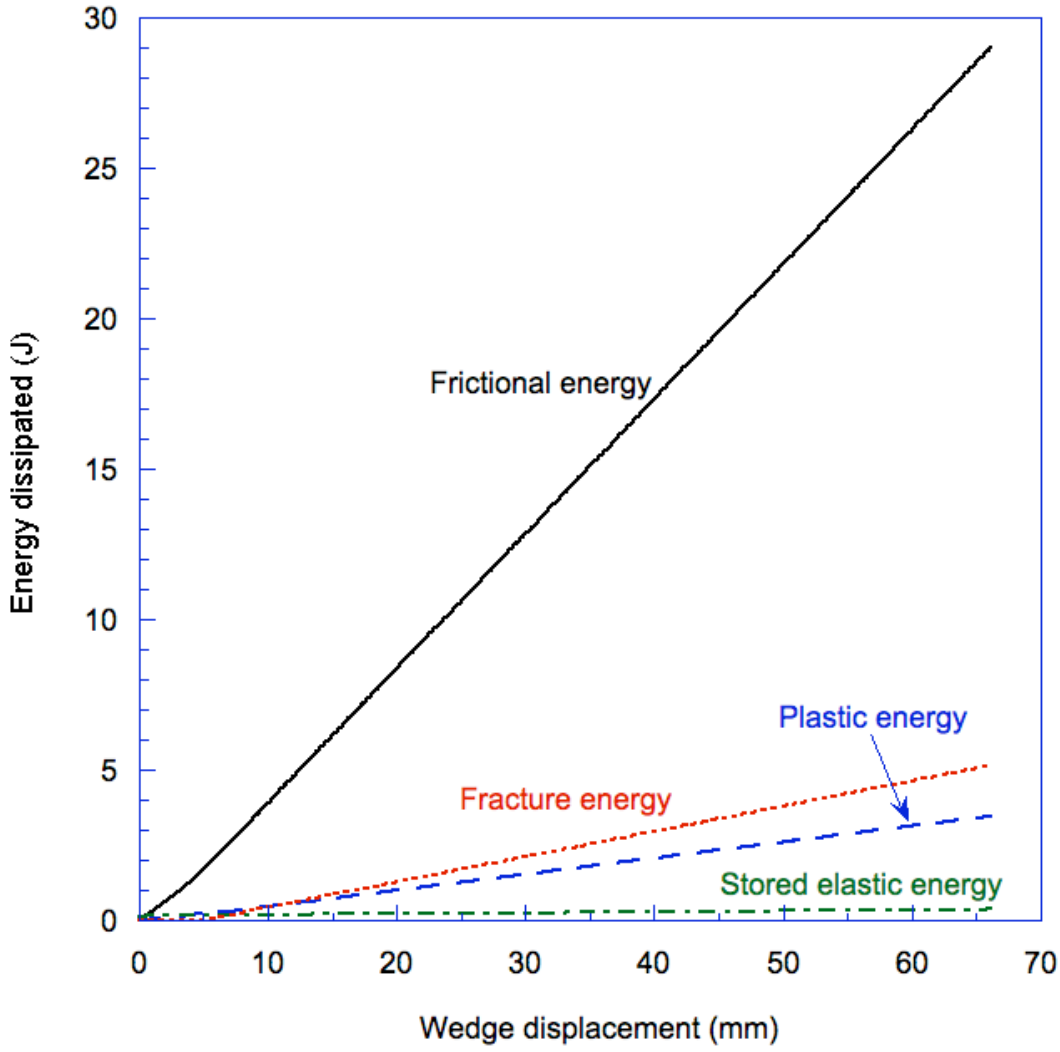


**Figure 11** The results of a numerical calculation for a quasi-static wedge test with a coefficient of friction equal to 0.32. The plots show how the elastic energy stored in the geometry, the plastic energy dissipated, the fracture energy dissipated and the frictional energy dissipated vary with wedge displacement.

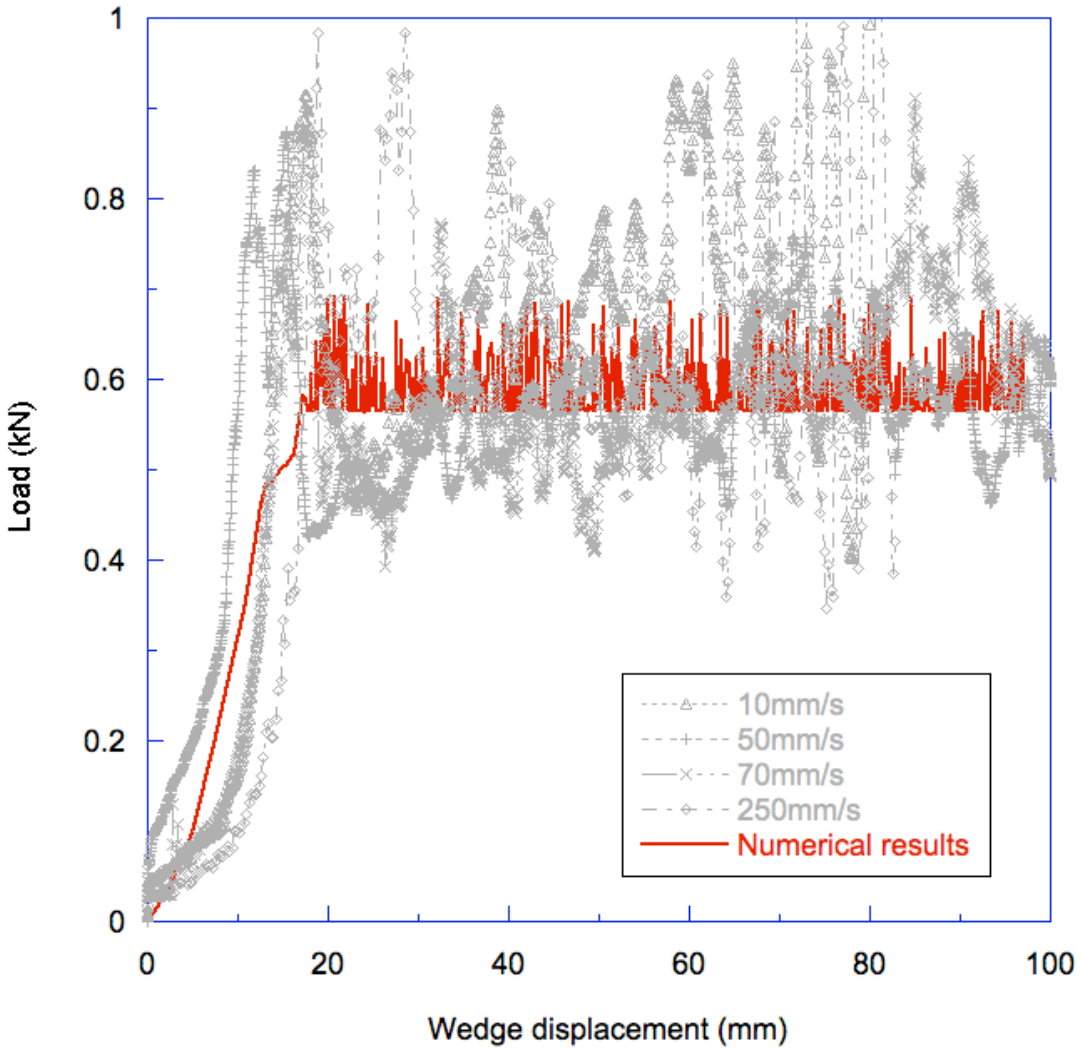


**Figure 12** A comparison between the reaction load on the wedge computed for the quasi-static tests with a coefficient of friction equal to 0.32, and loads measured during quasi-static tests.

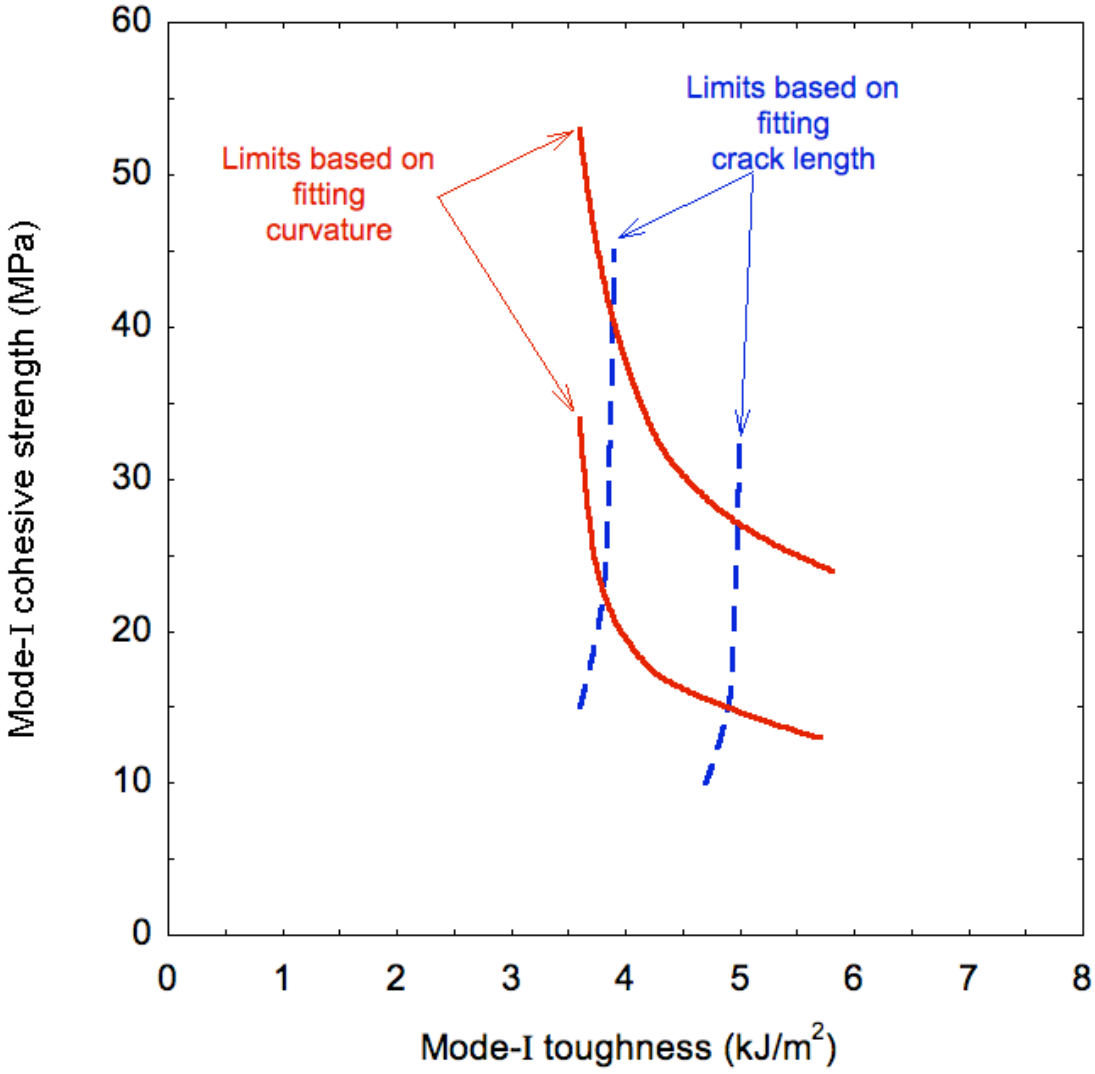


**Figure 13** A plot showing the ranges of values for the mode-I toughness and cohesive strength values that give an acceptable agreement between the results of numerical calculations, and the two experimental measurements that could be obtained from the wedge test.